DUET: Joint Deployment of Trucks and Drones for Object Monitoring

Lihao Wang*¶ Weijun Wang‡¶ Haipeng Dai* Jiaqi Zheng* Bangbang Ren† Shuyu Shi* Rong Gu*
*State Key Laboratory for Novel Software Technology, Nanjing University, Nanjing, Jiangsu 210024, CHINA
†National University of Defense Technology, Changsha, Hunan 410073, CHINA
‡Nanjing University, CHINA & University of Göttingen, GERMANY
Emails: Lihao_Wang@hotmail.com, wangalexweijun@gmail.com, {haipengdai, ssy, gurong}@nju.edu.cn,
jiaqi369@gmail.com, renbangbang11@nudt.edu.cn

***Abstract*—The limitation on the flight range motivates a hybrid monitoring system, wherein trucks carrying drones drive to pre-planned positions and then free drones for task execution. While the flight range limitation is mitigated, it is challenging to determine the destination of trucks and drones and set airborne cameras. This paper optimizes the joint Deployment of trUcks and dronEs for objecT monitoring (DUET), that is, deploy a set of trucks where each truck carries drones, and each drone is equipped with a varifocal camera such that the overall monitoring utility for target objects is maximized. To tackle the DUET problem, we first model the hybrid system and monitoring utility; then, discretize the solution space of DUET with performance bound. In this way, the problem is transformed into a two-level combinatorial optimization problem satisfying submodularity. To address it, a two-level greedy algorithm with $\frac{(e-1)^2}{e(2e-1)} \cdot (1-\epsilon)$ approximation ratio is proposed to select deployment strategies. After the strategy selection, an optimal method is devised to carefully adjust the strategy for energy saving and communication improvement without loss of monitoring utility. Both simulations and field experiments are conducted to evaluate the proposed framework, which outperforms baseline algorithms on monitoring utility by at least 28.4% and 40%, respectively.**

I. Introduction

With recent advances, drones or unmanned aerial vehicles (UAVs) are competent for monitoring tasks in different situations, and usually networked for area monitoring [1]. Especially, drone network enjoys an edge for its flexibility and low cost in temporary situations, *e.g.*, remote sensing after the disaster [2] and city patrol [3].

In this paper, we study the problem of Deployment of trUcks and dronEs for objecT monitoring (DUET). In our considered scenario, we have a given number of trucks, each of which carries a set of identical drones, and each drone is equipped with a varifocal camera. The coordinates of objects to monitor are known and fixed. The quality of captured pictures on an object by camera is defined as the quality of monitoring (QoM), and an object may have different QoM from different cameras. Once arriving at the given destination, the truck would release drones to monitor objects. The drones hover and trucks stall during the monitoring. The drones would fly back to the corresponding truck to get charged.

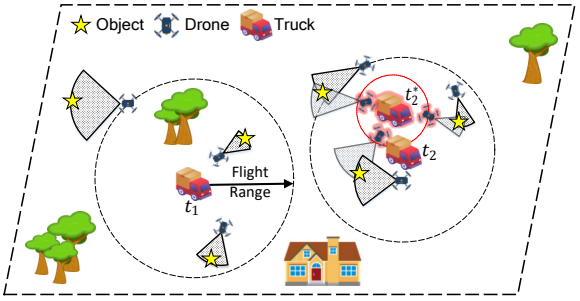

Fig. 1: Illustration of the DUET problem

Our task can be divided into two parts. The first part is to deploy the trucks and drones (including position, viewing orientation, and camera's focal length) elaborately such that the sum of fused QoM on every object, which is modelled as *monitoring utility* in Section III, is maximized. Note that we only consider the setting of airborne cameras and the destination of trucks and drones, when object positions and orientations are determined. Besides, we aim to deploy drones as close to their associated truck as possible because the distance between truck and drones influences the communication latency [4], [5], and a shorter distance means we can save more battery energy for monitoring tasks. Therefore, the second part of our task is to minimize the maximum distance between a truck and its carried drones after deployment while ensuring that the monitoring utility is not diminished.

Figure 1 shows an example of the DUET problem. We can observe that there are two trucks t_1 and t_2 (note that we still use t_1 and t_2 to denote their positions) on the plane, each of which carries three identical drones. The six drones have different viewing orientation and camera's focal length after deployment, and they monitor a total of six objects. To deploy them jointly, we first model the geometric constraints based on the mechanism of camera and the limitation on battery. Then we divide the area to extract solution space and select deployment strategies greedily afterwards. Further, for the truck t_2, it is more preferable to be deployed at position t_2^* rather than t_2, because the

Lihao Wang¶ and Weijun Wang¶ have equal contributions in this work. Haipeng Dai is the corresponding author.

978-1-6654-6824-4/22/$31.00 © 2022 IEEE

maximum distance between t_2^* and the associated three deployed drones (*i.e.* the radius of the red dotted circle, both of the truck at t_2^* and the drones are marked with red halo) is noticeably small than that between t_2 and the drones (the radius of the black dashed circle centered on t_2). Note that the three objects covered by the drones carried by t_2 remain monitored after the above deployment adjustment. Before further analysis, we first answer the following question.

Challenges in truck-drone system deployment. (1) The QoM affects the application of obtained images heavily [6]–[8]. We are the first to optimize QoM in the context of airborne varifocal camera, according to the survey. However, it is formidable to optimize the nonlinear QoM function for every airborne camera at the same time, let alone the aggregation of each QoM value. (2) The solution space of the DUET problem is continuous. Theoretically, there is an infinite number of candidate deployment positions for drones in a 2D plane. Worse still, the coupling of trucks and drones makes the solution space more complicated. Because of its high computational cost, the optimal algorithm which iterates the whole solution space is not applicable in practice. Besides, existing standard approaches which requires a given discrete solution space [9]–[11] do not work in DUET problem. (3) It is challenging to propose an approximation algorithm with a bounded gap to the optimal algorithm. Intuitively, the discrete solution space can be extracted by gridding the area. However, simply griding the area neglects objects position and camera parameters and its performance gap is hard to bound. (4) To improve the communication and save energy, a further adjustment is needed to narrow the distance between trucks and drones. To keep the monitoring utility maximized, the adjustment is limited under complicated geometric conditions. For a guaranteed performance, some common approaches, such as deep reinforcement learning [12], are not applicable.

Contributions. Our contributions can be summarized as follows. (1) For the first challenge, we quantify the quality of monitoring (QoM) and the monitoring utility with piecewise continuous functions firstly. Then we present a method to discretize the function with an approximation error bound; (2) For the second and third challenges, we prove that the problem is NP-hard firstly, and then propose a Maximal Object Set extraction method to reduce the continuous solution space into discrete solution space. A two-level greedy solution is derived based on it. We also analyze the approximation ratio and time complexity of the proposed algorithm; (3) For the fourth challenge, without loss of monitoring utility, we carefully adjust the obtained deployment strategies via a theoretically proved optimal method to minimize the Maximum Distance between a Truck and its carried Drones (MDTD) in a polynomial time complexity; (4) We conduct both simulation and field experiments to validate the proposed algorithm, where the proposed algorithm outperforms baselines on monitoring utility by at least 28.4% and 40%, respectively, and provide insights on the influence of different parameters.

To the best of our knowledge, we are the first to study the DUET problem. Although some existing related works consider joint deployment with drones, they only consider either jointly deploying trucks and drones for delivery applications [4], [13], or jointly deploying drones and locating drone base stations [9], [10], [14], which are quite different from DUET considering monitoring tasks. Moreover, their proposed solutions have no performance guarantee, while ours offer a constant approximation ratio. Besides, other related works, such as [15]–[22], consider camera sensor deployment, but none of them can be applied to address DUET because they never consider joint deployment issues.

II. Related Works

Joint deployment with drones. Major research efforts are dedicated to jointly deploying trucks and drones for delivery applications, and jointly deploying drones and drone base stations. For the former one, [23] proposes near-optimal algorithms to maximize delivery and sensing utility under drones energy constraints. [5] considers the networking technologies when routing trucks and drones. Further, Sung *et al.* in [24] presented a comprehensive review on the cutting edge approaches proposed for the above problem. For the latter one, Trotta *et al.* in [9] took the public transportation as base stations and maximized the system lifetime of a drone network with a heuristic algorithm. Hu *et al.* in [25] contributed an efficient algorithm to jointly optimize anchor point selection, path planning, and tour assignment for vehicle-drone cooperation with multiple drones. Ghazzai *et al.* in [10] employed the particle swarm optimization algorithm to determine the placement of drone docking stations. Liu *et al.* in [14] studied the problem to optimize the collected data size, geographic fairness, and the energy consumption simultaneously with given drone charging stations.

Generally, our work for the DUET problem is fundamentally different from the above literature in the following aspects: (1) DUET focuses on an unexplored scenario of jointly deploying trucks and drones for monitoring tasks; (2) DUET aims to maximize the monitoring utility, which is never studied before; and (3) we propose a constant approximation algorithms for DUET, but on the contrary, the above literature can hardly offer performance bound as they adopt techniques like heuristic algorithms [9] or machine learning techniques [14].

Camera sensor deployment. Deployment of camera sensors for monitoring tasks is well studied in the literature. For example, [15]–[18], [21], [26] study the deployment of camera sensors on a 2D plane. Specifically, Matthew *et al.* [17] modeled image quality and took the adjustment of zoom factor into consideration. Wang *et al.* in [15] modeled the anisotropic monitoring quality for airborne cameras. Liu *et al.* in [18] and Qi *et al.* in [21] selected both the deployment position and orientation of camera sensors. Wang *et al.* in [16] and Yu *et al.* in [26] took the barrier

TABLE I: Notations

Symbol	Meaning
t_l	the truck l, or its 2D coordinate
$c^i_{t_l}$	the drone i carried by the truck t_l, or its 2D coordinate
o_j	Object j to be monitored, or its 2D coordinate
K	Number of droness to be deployed
M	Number of truck to be deployed
P	Number of objects to be deployed
Ω	A 2D Plane
δ	The maximum range of drone
$\mathscr{f}$	The focal length of the camera
α	The angle of view of cameras
r	Farthest sight distance of camera
θ_j	Orientation angle of object o_j
$\psi^i_{t_l}$	Orientation angle of camera of drone $c^i_{t_l}$
$\mathscr{a}$	A single MEU
$\mathscr{A}$	MEU set
Γ	Set of candidate drone strategies
Λ	Set of candidate truck strategies

into consideration. Besides, Cao *et al.* in [22] and Wang *et al.* in [27] studied the camera sensor network in 3D space.

Unfortunately, none of the solutions above can address the DUET problem because all of them focus on the simple camera sensor network rather than the hybrid system. Also, the coupling of trucks and drones makes it infeasible to address DUET with simple variant of existing solutions.

Last but not least, we also surveyed other related work, such as deployment of wireless sensors [28], [29]. However, the problems studied in these literatures are different from the DUET problem. For example, [28] deploys wireless chargers, which leads to a different optimization objective from DUET. In addition, the proposed method in [28] is not applicable to the DUET problem due to different modeling on wireless sensors.

III. Problem Statement

A. Truck-drone System Model

Suppose that P objects $O = \{o_1, o_2, ..., o_P\}$ are distributed in a 2D plane to be monitored, and the orientation of each o_j is denoted by a unit vector $\overrightarrow{d_{o_j}}$. We use an angle θ_j in $[0, 2\pi)$ to denote the angle between the vector $\overrightarrow{d_{o_j}}$ and the x-axis. We have M trucks $T = \{t_1, t_2, ..., t_M\}$ and at most K drones carried by each to be deployed. The drones (each equipped with a camera) carried by the truck t_l is represented by a set $C_{t_l} = \{c^1_{t_l}, c^2_{t_l}, ..., c^K_{t_l}\}$ [1]. In the system model, the deployment of each drone (called a *strategy*) is described by a 4-tuple $(t_l, c^i_{t_l}, \psi^i_{t_l}, \mathscr{f}^i_{t_l})$, where $c^i_{t_l}$ is the position of the drone i carried by the truck t_l, $\psi^i_{t_l}$ is the viewing orientation angle of the i-th drone, and $\mathscr{f}^i_{t_l}$ is the focal length of the camera. For convenience, the orientation of the drone can also be represented by a unit vector $\overrightarrow{d_{c_i}}$.

[1] If no confusion arises, we also use t_l, $c^i_{t_l}$ and o_j to denote the position of trucks, drones, and objects respectively.

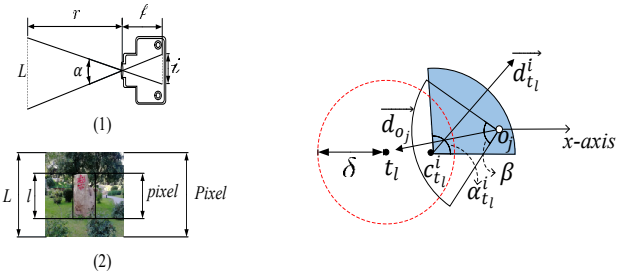

(a) Varifocal camera model (b) Object monitoring

Fig. 2: Model construction

We assume that every drone has the same battery capacity, *i.e.* equal (maximum) flight range, denoted by δ. Consequently, drones can fly inside a disk area centered on the truck's position with a radius of δ. We call the disk area Truck Supply Area (TSA). The truck can always charge the carried drones, and the energy consumption on communication can be ignored. Formally, for a truck t_l and its drone $c^i_{t_l}$, we have

$$\| t_l - c^i_{t_l} \| \le \delta. \tag{1}$$

The strategy of a truck is described with a 4-tuple $(t_l, C_{t_l}, \Psi_{t_l}, \mathscr{F}_{t_l})$, where C_{t_l} denotes the position set of the drones carried by a truck t_l, Ψ_{t_l} and $\mathscr{F}_{t_l}$ denotes the orientation set of drones and the focal length set of the cameras. Table I lists the notations we use in this paper.

B. Varifocal Camera Model

The varifocal camera model follows prior studies [30], [31]. Two factors determine the field of view of the camera model, *i.e.*, the angle of view (AoV) α and the range of distance r. Figure 2a visualizes the geometric relationship between parameters in a varifocal camera model. The relationship between AoV α and focal length $\mathscr{f}$ can be formulated as

$$\alpha = 2 \arctan \frac{\dot{\imath}}{2\mathscr{f}}, \tag{2}$$

where $\dot{\imath}$ is the size of the frame defined by the camera. As illustrated in Figure 2a, the relationship between the range of distance r and AoV α is

$$r = \frac{Pixel}{2 \cdot pixel} \cdot l \cdot z \cdot \cot \frac{\alpha}{2}, \tag{3}$$

where $Pixel$, $pixel$, l, and z denote the pixels of the entire image, the pixels of the object, the actual length of the object, and the zoom ratio of the camera, respectively.

C. Monitoring Quality

Following the prior work [17], [18] , the area monitored by a camera can be modeled as a sector shown in Figure 2b (painted area). On one hand, QoM distributes unevenly inside the sector in most cases; QoM varies along with the

distance d between camera and object and the focal length f of the camera. Based on the results of [17], $QoM \propto \frac{f^2}{d^2}$. On the other hand, QoM is limited by the angle between the facing orientation of the object and the viewing orientation of the camera; QoM would drop dramatically with the increment of this angle according to the results of [32]. To model this, we use *efficient angle* β, which is a constant parameter to the limitation between the facing orientation of the object and the viewing orientation of the camera when the object is monitored.

Following [33], we define that an object o_j facing $\overrightarrow{d_{o_j}}$ is monitored by a drone $c^i_{t_l}$, *iff.*: (1) o_j is inside the monitoring area of the camera carried by the drone $c^i_{t_l}$; (2) $A(\overrightarrow{d_{o_j}}, \overrightarrow{o_j c^i_{t_l}}) < \frac{\beta}{2}$, where $A(,)$ denotes the included angle between two vectors. For example, in Figure 2b, the object o_j is monitored with orientation $\overrightarrow{d_{o_j}}$. Note that $\psi^i_{t_l}$ and θ_j determine the directions of vector $d^i_{t_l}$ and d_{o_j}, respectively. Formally, the QoM for an object o_j monitored by a camera carried by drone $c^i_{t_l}$ can be described as

$$Q_f(o_j, t_l, c^i_{t_l}, \psi^i_{t_l}, f^i_{t_l}, \theta_j) = \begin{cases} \frac{\mu \cdot (f^i_{t_l})^2}{(||\overrightarrow{c^i_{t_l} o_j}|| + \nu)^2}, & 0 \le ||\overrightarrow{c^i_{t_l} o_j}|| \le r^i_{t_l}, \\ & \cos\frac{\alpha^i_{t_l}}{2} \le \frac{\overrightarrow{c^i_{t_l} o_j} \cdot \overrightarrow{d^i_{t_l}}}{||\overrightarrow{c^i_{t_l} o_j}||} \le 1, \\ & \cos\frac{\beta}{2} \le \frac{\overrightarrow{o_j c^i_{t_l}} \cdot \overrightarrow{d_{o_j}}}{||\overrightarrow{o_j c^i_{t_l}}||} \le 1, \\ 0, \quad otherwise. \end{cases} \tag{4}$$

where μ and ν are parameters determined by hardware and deployment environment. The distance $r^i_{t_l}$ and AoV $\alpha^i_{t_l}$ of the camera can be obtained with the focal length $f^i_{t_l}$ according to Equation (2) and (3).

D. Monitoring Utility

Before giving the definition of monitoring utility, the model needs to quantify the overlapped QoM for an object. We observe that when multiple drones monitor an object, the image with the maximum QoM would contain the complete information of all other images. For an object o_j with orientation θ_j, its total monitoring utility can be described with

$$U(T, o_j, \theta_j) = \max_{\substack{l=1,2,...,M, \\ i=1,2,...,K}} Q_f(o_j, t_l, c^i_{t_l}, \psi^i_{t_l}, f^i_{t_l}, \theta_j). \tag{5}$$

Note that we do not expect that every object is monitored. As to extensibility, our proof in Section IV-D shows that any function with submodularity is suitable as the utility function for our algorithm.

E. Problem Formulation

Assuming that the coordinates of the target object have been obtained, our task is to find out a joint deployment strategy of a given set of trucks and drones, such that the total monitoring utility of the P target objects is maximized.

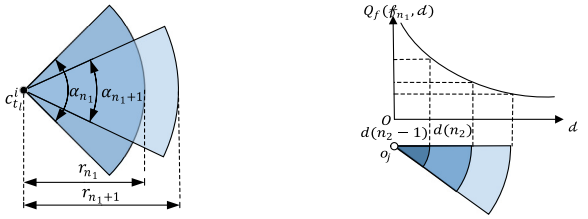

(a) Focal length discretization (b) Distance discretization

Fig. 3: QoM discretization

Formally, the Deployment of trUcks and DronEs for ObjecT Monitoring (DUET) problem is defined as follows:

$$\textbf{(P1)} \quad \max \quad \sum_{j=1}^{P} \max_{\substack{l=1,2,...,M, \\ i=1,2,...,K}} Q_f(o_j, t_l, c^i_{t_l}, \psi^i_{t_l}, f^i_{t_l}, \theta_j),$$
$$s.t. \quad f_{min} \le f_{c_i} \le f_{max}, \| t_l - c_i \| \le \delta, t_l, c^i_{t_l} \in \Omega,$$

where f_{min} and f_{max} control the variation range of focal length, and Ω denotes the plane that objects belong to.

Next, we have the following theorem.

***Theorem** 3.1:* The DUET problem is NP-hard.

We omit some proofs of theorems in this paper due to the space limit.

After we obtained the deployment, it is necessary to make adjustments such that the truck carried drones as close to the truck as possible because (1) the distance between truck and drones influences the communication latency [4], [5]; and (2) a shorter distance means we can save more battery energy for monitoring tasks. An optimal solution is proposed later in Section V to adjust the deployment.

IV. Solution

In this section, we design an approximation algorithm to transform the solution space from infinite to finite such that the original problem is transformed into a combinatorial optimization problem DUET-C (see Section IV-A to IV-C). Then, we propose a two-level greedy algorithm for DUET-C and bound both the approximation ratio and the time complexity of the whole algorithm (see Section IV-D).

A. Discretization of QoM

Given other parameters, we can use $Q_f(f, d)$ to describe the QoM function, where f denotes the focal length of the drone's camera, and d denotes the distance between the object and the drone, *i.e.*, $||\overrightarrow{c^i_{t_l} o_j}||$ in Equation (4). The core idea of QoM discretization is to divide the continuous QoM function into several intervals so that in each interval, the QoM value can be regarded as constant.

Specifically, we divide the focal length range $[f_{min}, f_{max}]$ into N_1 intervals $[f_0, f_1], (f_1, f_2], \ldots, (f_{N_1-1}, f_{N_1}]$, where $f_0 = f_{min}, f_{N_1} = f_{max}$. Define function $f(n_1) = f_{n_1}, 0 \le n_1 \le N_1$. In each interval $(f(n_1-1), f(n_1)]$, we use $f(n_1-1)$ to represent the focal length f falling in the interval. As is shown in Figure 3a, different focal length corresponds to

different AoV α and distance r. Similarly, we discretize $\mathscr{d}$ with $d(n_2), 0 \le n_2 \le N_2$, which is illustrated in Figure 3b.

After the discretization of $\mathscr{f}$ and $\mathscr{d}$, we get an approximated $\widetilde{Q_f}(\mathscr{f},\mathscr{d})$ of QoM function $Q_f(\mathscr{f},\mathscr{d})$:

$$\widetilde{Q_f}(\mathscr{f},\mathscr{d}) = \begin{cases} \widetilde{Q_f}(f(0),d(0)), & \mathscr{f} = f(0), \mathscr{d} = d(0), \\ \widetilde{Q_f}(f(n_1-1),d(n_2)), & f(n_1-1) < \mathscr{f} \le f(n_1), \\ & d(n_2-1) < \mathscr{d} \le d(n_2), \\ 0, & \mathscr{f} > f(N_1) \quad or \quad \mathscr{d} > d(N_2), \end{cases} \tag{6}$$

where $n_1 = 1,2,\ldots,N_1$ and $n_2 = 1,2,\ldots,N_2$.

With predetermined parameters ϵ_1 and ϵ_2, we have the following three theorems about the approximation errors of the QoM discretization.

***Theorem** 4.1:* With a given focal length $\mathscr{f} = \mathscr{f}_{n_1}$, let $d(n_2) = \nu((1+\epsilon_1)^{\frac{n_2}{2}} - 1), n_2 = 1,2,\ldots,N_2$, and $N_2 = \lceil \frac{2ln(\frac{\mathscr{d}_{max}}{\nu})+1}{ln(1+\epsilon_1)} \rceil$, we have the approximation error:

$$1 \le \frac{Q_f(\mathscr{f}_{n_1},\mathscr{d})}{\widetilde{Q_f}(\mathscr{f}_{n_1},\mathscr{d})} \le 1+\epsilon_1. \tag{7}$$

***Theorem** 4.2:* Given $d(n_2) = \nu((1+\epsilon_1)^{\frac{n_2}{2}} - 1), n_2 = 1,2,\ldots,N_2$, and $N_2 = \lceil \frac{2ln(\frac{\mathscr{d}_{max}}{\nu})+1}{ln(1+\epsilon_1)} \rceil$, let $f(n_1) = f(0) \cdot (\frac{1+\epsilon_2}{1+\epsilon_1})^{\frac{n_1}{2}}, n_1 = 1,2,\ldots,N_1$ and $N_1 = \lceil \frac{2ln(\frac{\mathscr{f}_{max}}{\mathscr{f}_{min}})}{ln(\frac{1+\epsilon_2}{1+\epsilon_1})} \rceil$, we have the approximation error:

$$1 \le \frac{Q_f(\mathscr{f},\mathscr{d})}{\widetilde{Q_f}(\mathscr{f},\mathscr{d})} \le 1+\epsilon_2. \tag{8}$$

***Theorem** 4.3:* Letting $\widetilde{U}(T,o_j,\theta_j)$ denote the total monitoring utility of the object o_j under $\widetilde{Q_f}(\mathscr{f},\mathscr{d})$, the approximation error is

$$1 \le \frac{U(T,o_j,\theta_j)}{\widetilde{U}(T,o_j,\theta_j)} \le 1+\epsilon_2, \tag{9}$$

where ϵ_2 is the same as that in Theorem 4.2.

B. Candidate Drone Strategy Extraction

In this subsection, we focus on extracting the candidate drone strategies for a single truck. The core idea is to divide the continuous 2D plane Ω into several discrete subareas so that wherever the drone locates in each subarea, the monitored objects sets are the same as each other.

Given the focal length $\mathscr{f}$ of all drone carried cameras, for truck t_l, the strategy of the i-th drone c^i is denoted by $(c^i, \psi^i_{t_l}, \mathscr{f})$, where c^i is the location of the drone and ψ^i is the direction of the drone. Then, we give two definitions.

***Definition** 4.1:* **(Dominance)** Given two drone strategies $(c^1,\psi^1,\mathscr{f}^1)$, $(c^2,\psi^2,\mathscr{f}^2)$, and their monitored sets of objects O_1 and O_2. If $O_1 = O_2$, $(c^1,\psi^1,\mathscr{f}^1)$ is equivalent to $(c^2,\psi^2,\mathscr{f}^2)$, or $(c^1,\psi^1,\mathscr{f}^1) \equiv (c^2,\psi^2,\mathscr{f}^2)$; If $O_1 \supset O_2$, $(c^1,\psi^1,\mathscr{f}^1)$ dominates $(c^2,\psi^2,\mathscr{f}^2)$, or $(c^1,\psi^1,\mathscr{f}^1) \succ (c^2,\psi^2,\mathscr{f}^2)$; And if $O_1 \supseteq O_2$, $(c^1,\psi^1,\mathscr{f}^1) \succeq (c^2,\psi^2,\mathscr{f}^2)$.

***Definition** 4.2:* **(Maximal Object Set (MOS))** Given a set of objects O_i monitored by a strategy $(c^i,\psi^i,\mathscr{f}^i)$, if there does not exist a strategy $(c^j,\psi^j,\mathscr{f}^j)$ such that $(c^j,\psi^j,\mathscr{f}^j)$ dominates $(c^i,\psi^i,\mathscr{f}^i)$, then O_i is a Maximal Coverage Set.

Algorithm 1: Drone Strategies Extraction

Input: a set O with P objects, the focal length $\mathscr{f}$ of carried cameras and 2D area Ω
Output: a set $\mathscr{A}^{\mathscr{f}}$ of divided subareas and a set $\Gamma^{\mathscr{f}}$ of candidate strategies for drones

1 $\mathscr{A}^{\mathscr{f}} = \emptyset$.
2 Compute the parameter α and r under focal length $\mathscr{f}$.
3 **for** *every object* $o_i \in O$ **do**
4 Draw the sector which represents the monitored model of object o_i and concentric arcs with radii of $d(1), d(2), \ldots, d(N_2)$ computed by QoM approximation approach inside the sector.
5 **for** *every two objects* $o_i \in O$ *and* $o_j \in O$ **do**
6 Draw a line connecting o_i and o_j which is extended to the boundaries of Ω. and two arcs passing through o_i and o_j with a circumference angle of $\alpha^{\mathscr{f}}$.
7 Record all divided subareas in $\mathscr{A}^{\mathscr{f}}$.
8 $\Gamma^{\mathscr{f}} = \emptyset$.
9 **for** *each divided subarea* $\mathscr{a}^{\mathscr{f}}_i$ *of* $\mathscr{A}^{\mathscr{f}}$ **do**
10 Select an arbitrary point c^* in the intersection area between $\mathscr{a}^{\mathscr{f}}_i$ and the TSA of truck t_l, where the drone is rotated from 0 to 2π. When the set of monitored objects is maximal, record the corresponding direction of the drone as ψ^*.
11 Add $(c^*,\psi^*,\mathscr{f})$ to $\Gamma^{\mathscr{f}}$.
12 Output the MEU set $\mathscr{A}^{\mathscr{f}}$ and candidate drone strategy set $\Gamma^{\mathscr{f}}$.

In order to extract the drone candidate positions, we divide the continuous 2D plane Ω into a set of MOS Equivalent Unit (MEU), in which drones have the same MOS set at any point; namely, all positions in the MEU are equivalent. Therefore, we only need to select one representative position inside the MEU as a candidate position for the drone. We present the details to obtain MEUs in Algorithm 1. Step 1-7 construct MEUs by leveraging lines and arcs (generated by monitoring sectors) dividing the 2D plane Ω. Step 8-12 extract the direction of drones. In particular, Algorithm 1 rotates the drone from 0 to 2π and records the direction monitoring the MOS. Since MOS always appears where a new (or covered) target object is included (or excluded) in the current monitored object set, Algorithm 1 checks whether it is MOS at these directions. In this way, we get the best direction $\psi^*_{t_l}$ of the drone c^*. Finally, we get every element $(c^*,\psi^*,\mathscr{f})$ of $\Gamma^{\mathscr{f}}$.

We present the following theorem about Algorithm 1.

***Theorem** 4.4:* The MOS set of a drone at any point in a given MEU is exactly the same.

C. Candidate Truck Strategy Extraction

In this subsection, we consider the deployment of trucks under a given focal length $\mathscr{f}$ after we have obtained the drone candidate strategy set $\Gamma^{\mathscr{f}}$ and the corresponding subarea set $\mathscr{A}$. Here, we use $(t_l, C_{t_l}, \Psi_{t_l}, \mathscr{f})$ to denote the strategy of truck t_l. To assist analysis, we present the following definition.

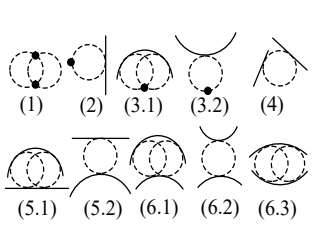

(a) Cases of critical geometric conditions for truck position extraction

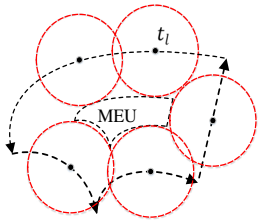

(b) An example of adjustment space for a truck

Fig. 4: Geometric insights

Algorithm 2: Truck strategies Extraction

Input: set of all MEUs $\mathscr{A}^{\ell}$, candidate drone strategy set Λ^{ℓ} and radius of TSA δ
Output: A set Λ^{ℓ} of all candidate truck strategies

1 $\Gamma^{\ell} = \emptyset$, $T = \emptyset$.
2 **for** *every MEU* a_i^{ℓ} *in* $\mathscr{A}^{\ell}$ **do**
3 Classify and record the boundary elements of a_i^{ℓ} into a set of end points S_p, a set of line segments S_l and a set of arcs S_a.
4 **for** *every combination between* S_p, S_l, *and* S_a **do**
5 Compute all feasible candidate truck deployment position and save in T.
6 **for** *every element* t_l *in* T **do**
7 Check whether the set of associated MEUs of t_l is the subset of those for other elements in Λ and remove t_l if so.
8 Construct strategy $(t_l, C_{t_l}, \Psi_{t_l}, \ell)$ based on the drone strategy of each associated MEUs and add $(t_l, C_{t_l}, \Psi_{t_l}, \ell)$ to Λ^{ℓ}.
9 Output Λ^{ℓ}.

***Definition** 4.3:* **(Associated MEU)** If a MEU is partially or entirely covered by the TSA of a truck deployment position t_l, we call it t_l's associated MEU.

Inspired by [29], we can determine the candidate truck strategies according to the critical geometric conditions between MEU and TSA. Briefly, if we move an arbitrary TSA in the 2D plane Ω, its MEU set changes iff. the TSA touches the boundary of a new MEU or leaves the boundary of an associated MEU. Recall that the boundary of a MEU consists of three elements: point, line segment, and arc. Figure 4a enumerates some possible cases of critical geometric conditions. For example, case (5.1) and (5.2) represents the condition where TSA is tangent to an arc and a line segment at the same time. Each geometric condition corresponds to one or two candidate truck deployment positions, and we can determine the set Λ^{ℓ} of candidate truck deployment positions in this way.

Formally, we present Algorithm 2. For each candidate truck deployment position t_l, we find out all the associated MEUs and determine the candidate drone strategy. With these candidate drone strategies, we obtain the candidate truck strategy $(t_l, C_{t_l}, \Psi_{t_l}, \ell)$.

Algorithm 3: Strategies Selection Algorithm

Input: candidate truck strategy set Λ, candidate drone strategy set Γ, objects set $O = \{o_1, o_2, \ldots, o_P\}$
Output: truck strategy set R and drone strategy set A.

1 Initialization: $\Delta(a|A_T) = h_1(A_T \cup \{a\}) - h_1(A_T)$, $\Delta(t|R) = h_2(R \cup \{t\})) - h_2(R)$.
2 $R = \emptyset$, $A = \emptyset$, $\Lambda' = \Lambda$.
3 **while** $|R| < M$ *and* $|\Lambda'| > 0$ **do**
4 **for** *each* $t_l \in \Lambda$ **do**
5 $\Gamma'_{t_l} = \Gamma_{t_l}$, $A_T = \emptyset$.
6 **while** $|A_T| < K$ *and* $|\Gamma'_{t_l}| > 0$ **do**
7 $a^* = argmax\{\Delta(a|A_T) | a \in \Gamma'_{t_l}\}$.
8 $A_T = A_T \cup \{a^*\}$.
9 $\Gamma'_{t_l} = \Gamma'_{t_l} \setminus a^*$.
10 $t^* = argmax\{\Delta(t|R) | t \in \Lambda'\}$.
11 $R = R \cup \{t^*\}$, $A = A \cup A_{t*}$, $\Lambda' = \Lambda' \setminus t^*$.
12 Output R and A.

We have the following theorem for Algorithm 2.

***Theorem** 4.5:* For any given truck deployment position t_x in the 2D plane Ω, there exists $t_l \in \Lambda^{\ell}$, such that t_x's associated MEU set is a subset of t_l's associated MEU set.

D. Problem Reformulation and Solution

Here, we consider the problem P1 where the focal length is adjustable. We first discretize the QoM function, and then employ Algorithm 1 to divide the 2D plane Ω and get the set $\mathscr{A} = \{\mathscr{A}^{\ell_0}, \mathscr{A}^{\ell_1}, \ldots, \mathscr{A}^{\ell_{N_1}}\}$. Taking $\mathscr{A}$ as the input, we extract the candidate truck positions set T via step 1-5 in Algorithm 2. For each candidate truck deployment position t_l, we determine the candidate drone strategies set Γ_{t_l} and generate the truck strategy Λ_{t_l} of the truck t_l via the step 6-8 in Algorithm 2. Note that the TSA of each truck candidate deployment position t_l may cover the MEU under different focal lengths. In this way, we reconstruct the solution space of the DUET problem with performance bound.

Then the DUET problem is transformed into a combinatorial optimization problem DUET-C, which can be decomposed into two subproblems. Letting A_T denote the set of selected truck strategies, the first subproblem is that for a truck strategy $(t_l, C_{t_l}, \Psi_{t_l}, \mathscr{F}_{t_l}) \in \Lambda \setminus A_T$, select a set with K candidate drone strategies from the candidate drone strategies set Γ_{t_l} such that the total monitoring utility of objects is maximized. Let x_i^1 denote a binary indicator about whether the i-th candidate drone strategy in Γ_{t_l} is selected, and the subproblem can be formulated with

$$\textbf{(P2-1)} \quad \max\ h_1(\Gamma_{t_l}) = \sum_{j=1}^{P} \Big(\max_{\substack{(t_l, c_{t_l}^i, \psi_{t_l}^i, \ell_{t_l}^i) \\ \in A_T \cup \Gamma_{t_l}}} x_i^1 \widetilde{Q_f}(o_j, t_l, c_{t_l}^i, \psi_{t_l}^i, \ell_{t_l}^i, \theta_j) \Big),$$

$$s.t. \quad \sum_{i=1}^{|\Gamma_{t_l}|} x_i^1 = K (x_i^1 \in \{0,1\}).$$

The other subproblem is that assuming each truck's strategies have been determined, select a set with M truck strategies from a set of candidate truck strategies Λ so that

the total monitoring utility of objects is maximized. Denote x_l^2 as a binary indicator about whether the lth candidate truck strategy in Λ is selected, and the subproblem can be formulated with

$$\textbf{(P2-2)} \quad \max\ h_2(\Lambda) = \sum_{j=1}^{P} \Big(\max_{\substack{(t_l, C_{t_l}, \Psi_{t_l}, \mathscr{F}_{t_l}) \\ \in \Lambda}} x_i^2 \widetilde{Q_f}(o_j, t_l, c_{t_l}^i, \psi_{t_l}^i, \mathscr{f}_{t_l}^i, \theta_j) \Big),$$
$$s.t. \quad \sum_{i=1}^{|\Lambda|} x_l^2 = M (x_l^2 \in \{0,1\}).$$

To address DUET-C, we propose a two-level greedy algorithm in Algorithm 3. In the case of no ambiguity, we use t to represent the truck candidate strategy with the deployment position at t. In each iteration, Algorithm 3 first greedily calculates K candidate drone strategies for each truck t_l in step 6-9. Next, from step 3 to step 11, the algorithm greedily selects the best M truck candidate strategies, and once the truck deployment strategy t^* is selected, the set A_{t*} of corresponding K selected drone candidate strategies is added to the set A.

We call Algorithm 1, Algorithm 2, and Algorithm 3 together as DUET algorithm. Then, we have the following theorem for the DUET algorithm.

***Theorem** 4.6:* Letting $\epsilon = \epsilon_2$, the approximation ratio of the DUET algorithm is $\frac{(e-1)^2}{e(2e-1)} \cdot (1-\epsilon)$, and its time complexity is $O(MKP^6 \epsilon_2^{-2} \sum_{i=0}^{6} P^{6-i} \epsilon_1^{-i})$.

Proof: According to the definition in [34], both $h_1(\Gamma_{t_l})$ and $h_2(\Lambda)$ are monotone submodular. Based on the previous theorems, we can see that only the approximation of QoM and Algorithm 3 contribute to the approximation ratio of DUET algorithm. According to [34], the approximation ratio for the one level greedy algorithm is $1 - \frac{1}{e}$.

Next, we denote set $R = \{t_1, t_2, \ldots, t_M\}$ as the candidate truck strategy set, and **OPT** as the optimal monitoring utility. Let both set $R(G,G)$ and set $R(O,G)$ select truck strategies greedily, while $R(G,G)$ selects drone strategies greedily and $R(O,G)$ selects drone strategies optimally. It is noteworthy that strategies in the two sets may not follow the same order because of the different selecting algorithms. Besides, for the i-th truck strategy t_i^{og} in $R(O,G)$, $\widetilde{t_i}^{og}$ means the drone strategies of t_i are selected greedily while the truck position t_i remains. $\Delta(t_i|R_{i-1})$ indicates the marginal increment of the monitoring utility when adding the truck strategy t_i into the strategy set R_{i-1}, which consists of $i-1$ selected truck strategies. $R(G,G)\,\&\,R(O,G)$ denotes the jointed set of the two selected truck strategy set with $R(G,G)$ and $R(O,G)$.

Firstly, when adding $\widetilde{t_i}^{og}$ in $R(O,G)$ to $R(G,G)$, we have $\Delta(t_i^{gg}|R_{i-1}(G,G)) \geq \Delta(\widetilde{t_i}^{og}|R_{i-1}(G,G))$ for the greedy property. Secondly, we have $\Delta(\widetilde{t_i}^{og}|R_{i-1}(G,G)) \geq \Delta(\widetilde{t_i}^{og}|R(G,G)\,\&\,R_{i-1}(O,G))$ because $h_2(\Lambda)$ is a monotone submodular function. Finally, for one level greedy algorithm, we have $\Delta(\widetilde{t_i}^{og}|R(G,G)\,\&\,R_{i-1}(O,G)) \geq (1-1/e)\cdot\Delta(t_i^{og}|R(G,G)\,\&\,R_{i-1}(O,G))$ with the approximation ratio of one level greedy algorithm. Therefore, we get

$$\Delta(t_i^{gg}|R_{i-1}(G,G)) \geq (1-1/e)\cdot\Delta(t_i^{og}|R(G,G)\,\&\,R_{i-1}(O,G)). \quad (10)$$

With accumulation, we have

$$\sum_{i=1}^{M} \Delta(t_i^{gg}|R_{i-1}(G,G)) \geq (1-1/e)\cdot\sum_{i=1}^{M}\Delta(t_i^{og}|R(G,G)\,\&\,R_{i-1}(O,G)). \quad (11)$$

Setting $\epsilon_3 = 1-1/e$, we have

$$(1+\epsilon_3)\sum_{i=1}^{M}\Delta(t_i^{gg}|R_{i-1}(G,G)) \geq \epsilon_3\cdot\sum_{i=1}^{M}\Delta(t_i^{gg}|R_{i-1}(G,G)) + \epsilon_3\cdot\sum_{i=1}^{M}\Delta(t_i^{og}|R(G,G)\,\&\,R_{i-1}(O,G)). \quad (12)$$

Further, since $h_2(R(G,G)) = \sum_{i=1}^{M}\Delta(t_i^{gg}|R_{i-1}(G,G))$, we have

$$h_2(R(G,G)) \geq \frac{\epsilon_3}{1+\epsilon_3}\cdot h_2(R(G,G)\,\&\,R(O,G)). \quad (13)$$

With the monotone submodularity of $h_2(\Gamma)$, we have

$$h_2(R(G,G)) \geq \frac{\epsilon_3}{1+\epsilon_3}\cdot h_2(R(O,G)). \quad (14)$$

According to [34], we have

$$h_2(R(G,G)) \geq \frac{\epsilon_3}{1+\epsilon_3}\cdot\epsilon_3\cdot\textbf{OPT} = \frac{(e-1)^2}{e(2e-1)}\cdot\textbf{OPT}. \quad (15)$$

According to Theorem 4.3, the approximation error brought by discretization is $1/(1+\epsilon_2)$, so the total approximation of the proposed DUET algorithm is $\frac{(e-1)^2}{e(2e-1)}\cdot 1/(1+\epsilon_2) \geq \frac{(e-1)^2}{e(2e-1)}\cdot(1-\epsilon_2) = \frac{(e-1)^2}{e(2e-1)}\cdot(1-\epsilon)$.

We omit the time complexity analysis to save space. ■

V. Deployment Adjustment

This section aims to adjust the position of drones and trucks obtained by the DUET algorithm so that for a truck t_l and the carried drones C_{t_l}, the Maximum Distance between a Truck and its carried Drones (MDTD) is minimized without loss of monitoring utility.

A. Adjustment Space for Truck and Drones

In this subsection, we will determine the adjustment space for trucks and drones. Obviously, we have to keep the TSA of truck t_l always associated with each MEU in the MEU set $\mathscr{A}_{t_l}^*$ selected by DUET algorithm.

As is shown in Figure 4b, for a selected MEU a_i, we move the corresponding TSA around a_i's boundary and keep the TSA tangent to a_i during the process. Then, as long as the truck is deployed inside the area enclosed by the moving trajectory of TSA's center, the TSA corresponding to t_l can always keep associated with the MEU a_i. For K selected MEUs, we obtain the corresponding enclosed area of each MEU. The intersection of them is called the truck alternative deployment area, denoted as $\mathscr{T}$.

For drones carried by truck t_l, the adjustment space is the intersection area between the corresponding MEU and the TSA. We denote the TSA of t_l as TSA_{t_l}, one selected

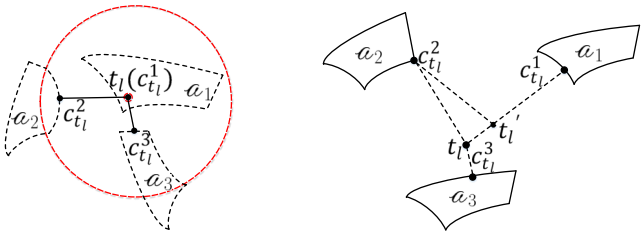

(a) Position adjustment sample (b) Auxiliary figure for Theorem 5.1

Fig. 5: Illustration for position adjustment

MEU associated with t_l as a_i and the drone corresponding to a_i as $c^i_{t_l}$. The extended problem is formulated as:

$$\textbf{(P3)} \quad \min \max_{i=1,2,\ldots,|C_{t_l}|} \|t_l - c^i_{t_l}\|,$$
$$s.t. \quad t_l \in \mathcal{T}, c^i_{t_l} \in a_i \cap TSA_{t_l}.$$

B. Alternative Position Extraction and Solution

In this subsection, we extract the finite solution space of adjustment for trucks and drones. Firstly, we consider the adjustment of drones. If $t_l \in a_i$, we set the position of $c^i_{t_l}$ to the position of t_l. Otherwise, the nearest point to t_l in a_i must lie on the boundary of a_i. The nearest point can be obtained easily since the boundary of a_i is made up of arcs and line segments. For example, in Figure 5a, we choose $c^1_{t_l}$, $c^2_{t_l}$, and $c^3_{t_l}$ as the drone alternative positions.

Process each element, *i.e.*, line segment and arc, of a_i's boundary, and we get the nearest point to t_l in a_i and the shortest distance between truck and drone. In fact, the nearest point to t_l is also the optimal drone position for adjustment. Without ambiguity, we denote $a^\#_i, i = 1,\ldots,K$ as the MEU where the ith farthest alternative drone position to t_l lies, and $L_i(t_l)$ as the shortest distance from t_l to $a^\#_i$ in the following part.

Then, we consider the adjustment of trucks. We present two geometric conditions satisfied by the optimal solution to reduce the solution space $\mathcal{T}$ in the following theorems.

***Theorem** 5.1:* For a truck position t_l adjusted by the optimal algorithm, the farthest drone from t_l and the second-farthest drone from t_l have the same distance to the truck.

Denoting e_3 as the truck trajectory that satisfies Theorem 5.1, and ℓ_i as the shortest distance between a_i and e_3, where $i = 1,2,\ldots,K$, we have the following theorem.

***Theorem** 5.2:* For an optimal truck position p on e_3, supposing the nearest point in a_1 to p lies on e_1 and the nearest point in a_2 to p lies on e_2, the point p satisfies either $L_1(p) = \ell_1$, or $L_1(p) = L_3(p)$.

With the two theorems above, we calculate the alternative truck positions and add them into $\mathcal{P}$, which denotes the set of truck alternative positions. Then, we iterate $\mathcal{P}$, adjust drones and determine the optimal solution. Obviously, our solution is polynomial-time complexity. We call DUET algorithm using deployment adjustment as DUET+.

VI. Simulation Results

A. Evaluation setup

In our simulation, objects are uniformly distributed in a 4000×4000 square space, and the orientations of objects are randomly selected from $[0,2\pi]$. If no otherwise stated, we set $P = 21$, $M = 10$, $K = 2$, $\delta = 500$, $\epsilon_1 = 0.25$, $\epsilon_2 = 0.5$, $\beta = \pi/6$, $\iota = \sqrt{3}$, $\frac{Pixel}{pixel}\cdot l\cdot z = \frac{10}{\sqrt{3}}$, $\ell \in [\frac{3}{2}, \frac{\sqrt{3}}{4-2\sqrt{3}}]$, respectively. The above settings let the camera model vary in $\alpha \in [\pi/6, \pi/3]$ and $r \in [5, 10.78]$. Each data point in the figures stands for the averaging results of at least 20 random instances.

Since there is no other existing algorithm for DUET, we propose four algorithms for comparison: Random Random Algorithm (RR); Random Greedy Algorithm (RG), which is adapted from [35]; Greedy Random Algorithm (GR); and Grid Greedy Algorithm (GGG), which is adapted from [15]. Specifically, RR, RG, and GR extract solution space in the same way as DUET. RR selects both drone strategies and truck strategies randomly. RG selects drone strategies greedily while selecting truck strategies randomly. GR selects drone strategies randomly while selecting truck strategies greedily. GGG first meshes the deployment area and then greedily selects both truck deployment locations and drone deployment positions from the grid points. On the premise of ensuring that at least one object is monitored, the camera parameters of each drone are initialized randomly.

On deployment adjustment, we also present two comparison algorithms, *i.e.*, Random and Grid, to DUET+. Random makes no adjustments, while Grid selects positions greedily after meshing the space.

B. Performance Comparison

1) Impact of Number of Objects P: Our simulation results show that, on average, DUET outperforms RR, RG, GR, and GGG by 702%, 525%, 35.7%, and 28.4%, respectively, in terms of P. As is shown in Figure 6, the increasing gap between DUET and other algorithms means DUET algorithm can make a better deployment of trucks and drones with more objects.

2) Impact of the maximum range of drone δ: Our simulation results show that, on average, DUET outperforms RR, RG, GR, and GGG by 754%, 554%, 44.2%, and 40.9%, respectively, in terms of δ. From Figure 7, we can see that similar to the impact of P, as the range of the drone increases, the candidate drone strategy set of a truck increases. Considering that GR selects drone strategies randomly, this is a possible reason for the curve of GR, which changes from increasing to decreasing.

3) Performance of Position Adjustment: Our simulation results show that, on average, our proposed adjustment method DUET+ outperforms Random and Grid by 78% and 70%, respectively. As is shown in Figure 8, the MDTD of our adjustment is close to zero from truck 4 to truck 10. The experimental result is consistent with the conclusion that our adjustment provides an optimal solution.

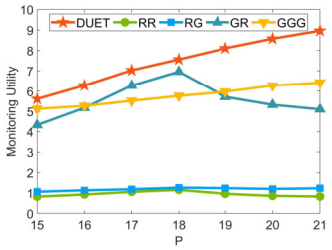

Fig. 6: P vs. utility

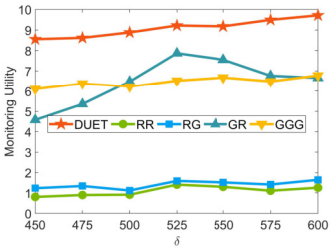

Fig. 7: δ vs. utility

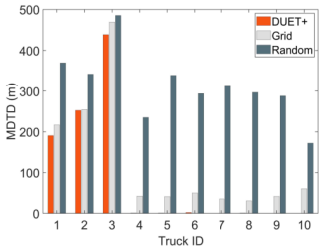

Fig. 8: MDTD of each truck

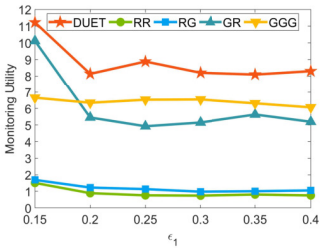

Fig. 9: ϵ_1 vs. utility

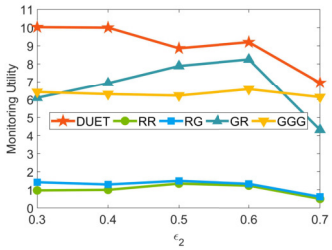

Fig. 10: ϵ_2 vs. utility

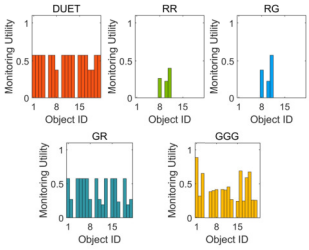

Fig. 11: Object utility

Fig. 12: A nameplate sample

Fig. 13: Nameplate Distribution

C. Insights

Here we study the impact of approximation errors ϵ_1 and ϵ_2 on monitoring utility. For one thing, in terms of ϵ_1, our simulation results show that, on average, DUET outperforms RR, RG, GR, and GGG by 907%, 656%, 50.5%, and 37.2%, respectively. For another thing, in terms of ϵ_2, our simulation results show that on average, DUET outperforms RR, RG, GR, and GGG by 866%, 679%, 38.7%, and 42.1%, respectively. From Figure 9 and Figure 10, the comparison between two curve trends under ϵ_1 and ϵ_2 indicates that DUET is more sensitive to the approximation error ϵ_2 than ϵ_1, which is consistent with our theoretical analysis of DUET. Besides, note that the gap between DUET and GR narrows with increasing ϵ_2, which may be caused by the shrinkage of the candidate solution set. We also present a more detailed monitoring utility distribution in Figure 11. We can see that DUET distributes the monitoring utility of each object more evenly and achieves better fairness. This advantage improves the overall monitoring utility.

VII. Field Experiments

Experimental setup. To evaluate the DUET+ algorithm, a field testbed is built to monitor the walls of buildings so that problems like peeling off could be found out. Here, we choose the nameplate as the target object of 11 buildings, *i.e.*, $P = 11$, which distribute in an area of $1200\,m \times 1000\,m$. Figure 12 shows an example of the nameplate and the distribution of nameplates is shown in Figure 13. Each drone would take a picture of the nameplate, and then we feed the obtained photos to the state-of-the-art recognition model proposed in [36]. We use edit distance [37] to determine whether the recognized text and the ground truth

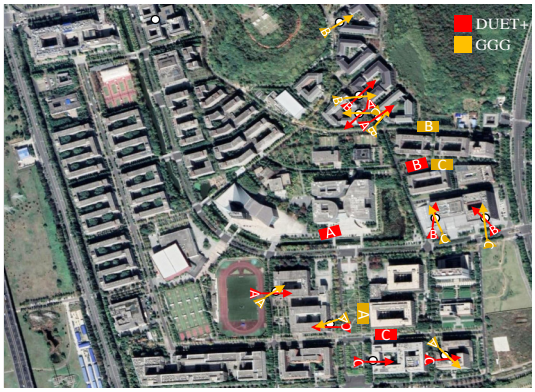

Fig. 14: Distribution of trucks and drones

are approximately the same. A nameplate is recognized if the minimum edit distance to the ground truth is less than a threshold. The networking part of the testbed consists of 3 trucks, and each truck carries 3 drones. Besides, we set $\delta = 300$, $\beta = \pi/6$, $\epsilon_1 = 0.25$, and $\epsilon_2 = 0.5$. To validate DUET+, we compare its results with the GGG algorithm.

Experimental results. Figure 14 illustrates the deployment results for DUET+ and GGG, where the triangle represents the drone position, and the rectangle represents the truck position. The truck and its drones share the same letter. In general, DUET+ outperforms GGG by 51.6% in monitoring utility and 40.0% in recognition accuracy. We can see that due to the limitation of flight range, the outlier (point 3) is dropped by both algorithms. In addition, for nameplates recognized only by DUET+, the monitoring utility of DUET+ is higher than GGG, which indicates that the DUET+ algorithm helps improve the recognition accuracy in real applications.

VIII. Conclusion

This paper proposes an innovative algorithm for the deployment of a truck-drone hybrid system to maximize the monitoring utility in a polynomial time, and meanwhile minimize the flight range of drones. The key technical depth is in extracting the discrete candidate strategies set of the optimization problem from the continuous solution space by an approximated geometric method with a performance guarantee, and keeping trucks and drones as close as possible. With finite solution space, the optimization problem is addressed through a two-level greedy algorithm with a bounded overall approximation ratio. Then, an optimal algorithm is proposed to tune the deployment arrangements. Our evaluation results show that our scheme outperforms comparison algorithms by at least 28.4% in simulation and 40% in field experiments.

Acknowledgment

This work was supported in part by the National Natural Science Foundation of China under Grant 61872178, 61832005, 62172206, 62072230, U1811461 and 61902177, in part by the Natural Science Foundation of Jiangsu Province of China under number BK20190298, in part by the Collaborative Innovation Center of Novel Software Technology and Industrialization, Nanjing University, and in part by the Jiangsu High-level Innovation and Entrepreneurship (Shuangchuang) Program.

References

[1] L. Gupta, R. Jain, and G. Vaszkun, "Survey of important issues in uav communication networks," *IEEE Communications Surveys Tutorials*, vol. 18, no. 2, pp. 1123–1152, 2016.

[2] M. Ishigami and T. Sugiyama, "A novel drone's height control algorithm for throughput optimization in disaster resilient network," *IEEE Transactions on Vehicular Technology*, vol. 69, no. 12, pp. 16 188–16 190, 2020.

[3] Y. Fan, S. Chu, W. Zhang, R. Song, and Y. Li, "Learn by observation: Imitation learning for drone patrolling from videos of a human navigator," in *IEEE/RSJ IROS*, 2020.

[4] D. Wang, P. Hu, J. Du, P. Zhou, T. Deng, and M. Hu, "Routing and scheduling for hybrid truck-drone collaborative parcel delivery with independent and truck-carried drones," *IEEE Internet of Things Journal*, vol. 6, no. 6, pp. 10 483–10 495, 2019.

[5] M. Patchou, B. Sliwa, and C. Wietfeld, "Unmanned aerial vehicles in logistics: Efficiency gains and communication performance of hybrid combinations of ground and aerial vehicles," in *IEEE VNC*, 2019.

[6] S. Yogamani, C. Hughes, J. Horgan, G. Sistu, S. Chennupati, M. Uricar, S. Milz, M. Simon, K. Amende, C. Witt, H. Rashed, S. Nayak, S. Mansoor, P. Varley, X. Perrotton, D. Odea, and P. Pérez, "Woodscape: A multi-task, multi-camera fisheye dataset for autonomous driving," in *IEEE/CVF ICCV*, 2019.

[7] C. Lu, Y. Chang, and W. Chiu, "Bridging the visual gap: Wide-range image blending," in *IEEE CVPR*, 2021.

[8] A. Raj, M. Zollhöfer, T. Simon, J. Saragih, S. Saito, J. Hays, and S. Lombardi, "Pixel-aligned volumetric avatars," in *IEEE CVPR*, 2021.

[9] A. Trotta, F. D. Andreagiovanni, M. Felice, E. Natalizio, and K. R. Chowdhury, "When uavs ride a bus: Towards energy-efficient city-scale video surveillance," in *IEEE INFOCOM*, 2018.

[10] H. Ghazzai, H. Menouar, A. Kadri, and Y. Massoud, "Future uav-based its: A comprehensive scheduling framework," *IEEE Access*, vol. 7, pp. 75 678–75 695, 2019.

[11] T. Kimura and M. Ogura, "Distributed collaborative 3d-deployment of uav base stations for on-demand coverage," in *IEEE INFOCOM*, 2020.

[12] X. Huang, S. Leng, S. Maharjan, and Y. Zhang, "Multi-agent deep reinforcement learning for computation offloading and interference coordination in small cell networks," *IEEE Transactions on Vehicular Technology*, vol. 70, no. 9, pp. 9282–9293, 2021.

[13] G. Wu, M. Fan, J. Shi, and Y. Feng, "Reinforcement learning based truck-and-drone coordinated delivery," *IEEE Transactions on Artificial Intelligence*, 2021.

[14] C. H. Liu, C. Piao, and J. Tang, "Energy-efficient uav crowdsensing with multiple charging stations by deep learning," in *IEEE INFOCOM*, 2020.

[15] W. Wang, H. Dai, C. Dong, F. Xiao, J. Zheng, X. Cheng, G. Chen, and X. Fu, "Deployment of unmanned aerial vehicles for anisotropic monitoring tasks," *IEEE Transactions on Mobile Computing*, vol. 21, no. 2, pp. 495–513, 2022.

[16] W. Yi and G. Cao, "Barrier coverage in camera sensor networks," in *ACM MobiHoc*, 2011.

[17] M. P. Johnson and A. Barnoy, "Pan and scan: Configuring cameras for coverage," in *IEEE INFOCOM*, 2011.

[18] Z. Liu and G. Jiang, "Sensor parameter estimation for full-view coverage of camera sensor networks based on bounded convex region deployment," *IEEE Access*, vol. 9, pp. 97 129–97 137, 2021.

[19] S. Aghajanzadeh, R. Naidu, S.-H. Chen, C. Tung, A. Goel, Y.-H. Lu, and G. K. Thiruvathukal, "Camera placement meeting restrictions of computer vision," in *IEEE ICIP*, 2020.

[20] A. Saeed, A. Abdelkader, M. Khan, A. Neishaboori, K. A. Harras, and A. Mohamed, "Argus: Realistic target coverage by drones," in *ACM/IEEE IPSN*, 2017.

[21] Q. Zhang, S. He, and J. Chen, "Toward optimal orientation scheduling for full-view coverage in camera sensor networks," in *IEEE GLOBECOM*, 2016.

[22] B. Cao, M. Li, X. Liu, J. Zhao, W. Cao, and Z. Lv, "Many-objective deployment optimization for a drone-assisted camera network," *IEEE Transactions on Network Science and Engineering*, vol. 8, no. 4, pp. 2756–2764, 2021.

[23] C. Xiang, Y. Zhou, H. Dai, Y. Qu, S. He, C. Chen, and P. Yang, "Reusing delivery drones for urban crowdsensing," *IEEE Transactions on Mobile Computing*, pp. 1–1, 2022 (Early Access).

[24] S. H. Chung, B. Sah, and J. Lee, "Optimization for drone and drone-truck combined operations: A review of the state of the art and future directions," *Computers & Operations Research*, vol. 123, p. 105004, 2020.

[25] M. Hu, W. Liu, K. Peng, X. Ma, W. Cheng, J. Liu, and B. Li, "Joint routing and scheduling for vehicle-assisted multidrone surveillance," *IEEE Internet of Things Journal*, vol. 6, no. 2, pp. 1781–1790, 2019.

[26] Z. Yu, Y. Fan, T. Jin, A. C. Champion, and X. Dong, "Local face-view barrier coverage in camera sensor networks," in *IEEE INFOCOM*, 2015.

[27] W. Wang, H. Dai, C. Dong, X. Cheng, X. Wang, P. Yang, G. Chen, and W. Dou, "Placement of unmanned aerial vehicles for directional coverage in 3d space," *IEEE/ACM Transactions on Networking*, vol. 28, no. 2, pp. 888–901, 2020.

[28] H. Dai, C. Wu, X. Wang, W. Dou, and Y. Liu, "Placing wireless chargers with limited mobility," in *IEEE INFOCOM*, 2020, pp. 2056–2065.

[29] H. Dai, X. Wang, X. Lin, R. Gu, S. Shi, Y. Liu, W. Dou, and G. Chen, "Placing wireless chargers with limited mobility," *IEEE Transactions on Mobile Computing*, pp. 1–1, 2021.

[30] Jacobson and R. Eric, "The manual of photography," *Focal Press*, 2000.

[31] F. Li, Z. Sun, A. Li, B. Niu, and G. Cao, "Hideme: Privacy-preserving photo sharing on social networks," in *IEEE INFOCOM*, 2019.

[32] M. Kan, S. Shan, and X. Chen, "Multi-view deep network for cross-view classification," in *IEEE CVPR*, 2016.

[33] Y. Wu, Y. Wang, W. Hu, and G. Cao, "Smartphoto: A resource-aware crowdsourcing approach for image sensing with smartphones," *IEEE Transactions on Mobile Computing*, vol. 15, no. 5, pp. 1249–1263, 2016.

[34] S. Fujishige, *Submodular functions and optimization*, 2005.

[35] W. Wang, H. Dai, C. Dong, X. Cheng, and W. Dou, "Panda: Placement of unmanned aerial vehicles achieving 3d directional coverage," in *IEEE INFOCOM*, 2019.

[36] Y. Du, C. Li, R. Guo, X. Yin, W. Liu, J. Zhou, Y. Bai, Z. Yu, Y. Yang, Q. Dang, and H. Wang, "Pp-ocr: A practical ultra lightweight ocr system," 2020.

[37] C. Manning, P. Raghavan, H. Schtextbackslashütze, and E. Corporation, *Introduction to Information Retrieval*, 01 2008, vol. 13.